CHAPTER 3

ARTICLE FOR SUBMISSION

Chapter 3 comprises the manuscript of an article submitted to the European Journal of Pharmaceutical Sciences. The article presents the Introduction, Material and methods, Results, Discussion and Conclusion of the synthesised antimalarial compounds of this study. This article is prepared according to the author's guidelines, available in the author information pack on the Journal's homepage:

http://www.elsevier.com/journals/european-journal-of-pharmaceutical-sciences/0928-0987/guide-for-authors

European Journal of Pharmaceutical Sciences 56 (2014) 16–27

Contents lists available at ScienceDirect

European Journal of Pharmaceutical Sciences

journal homepage: www.elsevier.com/locate/ejps

Synthesis and *in vitro* biological evaluation of aminoacridines and artemisinin–acridine hybrids

Juan P. Joubert [a], Frans J. Smit [a], Lissinda du Plessis [b], Peter J. Smith [c], David D. N'Da [b,*]

[a] Department of Pharmaceutical Chemistry, North-West University, Potchefstroom 2520, South Africa
[b] Centre of Excellence for Pharmaceutical Sciences (PHARMCEN), North-West University, Potchefstroom 2520, South Africa
[c] Department of Pharmacology, University of Cape Town, Groote Schuur Hospital, Observatory 7925, South Africa

ARTICLE INFO

Article history:
Received 4 December 2013
Received in revised form 13 January 2014
Accepted 29 January 2014
Available online 18 February 2014

Keywords:
Malaria
Artemisinin
Acridine
Hybrids
Cytotoxicity
Apoptosis

ABSTRACT

During this study, 9-aminoacridine and artemisinin–acridine hybrid compounds were synthesized and the *in vitro* for antimalarial activity against both the chloroquine sensitive but also gametocytocidal strain (NF54), and chloroquine resistant (Dd2) strains of *Plasmodium falciparum* was determined. *In vitro* cytotoxicity against CHO cells, apoptosis of HepG2 and SH-SY5Y as well as anticancer activity against HeLa cell lines were assessed. The hybrids were synthesized, using a microwave-assisted radiation method by covalently linking artemisinin and acridine pharmacophores by means of a liable, aminoethyl ether linker. The synthesized compounds were found active against both the *Plasmodium* strains and displayed superior selective toxicity towards the parasitic cells. Hybrid **7**, however, containing ethylenediamine linker, proved the most active of all of the synthesized compounds. It had seven-fold higher antigametocytocidal activity compared to chloroquine and was also found to be seven-fold more potent than chloroquine against the Dd2 strain, with highly selective action towards the parasitic cells. This hybrid also showed favourable anti-cancer activity against the HeLa cells, three- and eight-fold higher than those of chloroquine and melphalan, respectively. This hybrid may therefore stand as drug candidate for further investigation in the search for new and effective drugs against malaria and cervical cancer.

1. Introduction

Malaria is a life threatening disease to 3.3 billion people globally, of which predominantly children under the age of five, pregnant women, geriatrics and immunocompromized individuals (WHO, 2012) are at risk of contracting it. In 2011, the estimated malaria related deaths were 660,000 out of 219 million reported cases. 81% of these cases and 91% of malaria related mortality occurred in the African region (WHO, 2011). As infectious disease, malaria accounts for the second highest death rate in Africa, following HIV/Aids, whilst malaria comprizes the fifth deadliest disease, worldwide (Global Malaria action Plan, 2008).

The armamentariums, currently used to treat malaria, are from seven drug classes, namely 4-aminoquinolines (chloroquine), arylaminoalcohols, 8-aminoquinolines, artemisinins (Fig. 1), antifolates, hydroxynaphthoquinones, inhibitors of the respiratory chain and antibiotics (Rudrapal, 2011; Schlitzer, 2008). The ideal malaria pharmacotherapy should preferably be a cost effective and easily obtainable monotherapy. However, the malaria parasite's intrinsic ability to attain drug resistance through various mechanisms (Gregson and Plowe, 2005), has rendered traditionally used antimalarial drugs, such as chloroquine, (CQ) therapeutically ineffective, whilst having elevated the artemisinins as the only viable first line treatment option for uncomplicated *P. falciparum*.

Artemisinin therapeutic proficiency is limited by its low solubility in both oil and water and by its short plasma half-life, which had paved the way for the synthesis of semi-synthetic drugs with superior pharmacological properties (Ploypradith, 2004). Despite these improved properties of the semi-synthetic derivatives, the artemisinins, as a class, still possess clear disadvantages, *viz.* short half-lives, irregular absorption, liability towards acid hydrolysis, increased dosage frequency and high recrudescence, all of which prohibit their use as monotherapy (Meshnick, 2002; Price et al., 1996). These shortcomings restrict therapeutic efficacy, patient compliance and increase the possible development of drug resistance.

Efforts to enhance their efficiency and to avoid the development of parasitic resistance to the artemisinin class, had led to the incorporation of a partner drug that meets with preordained specifications to the artemisinins, resulting in artemisinin based combination therapies (ACTs). ACTs combine fast acting, highly potent

* Corresponding author. Tel.: +27 18 299 2256; fax: +27 18 299 4243.
E-mail address: david.nda@nwu.ac.za (D.D. N'Da).

http://dx.doi.org/10.1016/j.ejps.2014.01.014
0928-0987/

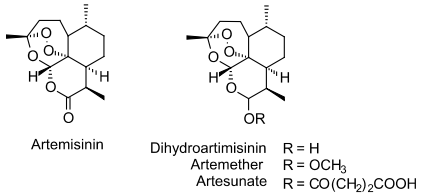

Fig. 1. Structures of artemisinins. The artemisinins class comprises artemisinin and its oil-soluble semi-synthetic derivatives dihydroartemisinin, artemether and arteether, and water-soluble, artesunate.

artemisinin derivatives with a longer acting partner drug from another class. In that combination, the short acting, highly potent artemisinin derivative reduces the parasitemia, after which the slower, eliminated partner compound prevents parasite recrudescence (Price, 2013). The World Health Organization (WHO) recommends ACTs as first line treatment for uncomplicated *P. falciparum* malaria (Amuasi et al., 2012; Fink et al., 2013). However, artemisinins' tolerance has already been confirmed through prolonged, parasite clearance times, despite adequate drug exposure in the Greater Mekong countries, like Cambodia, Myanmar, Thailand and Vietnam (Fairhurst et al., 2012). This worrying predicament can have dire consequences, since the artemisinin class serves as the foundation for current treatment regimes, thus emphasizing the urgent search for new and effective therapies to be identified and developed.

A new approach to impede drug resistance development is the synthesis of hybrid molecules (Burgess et al., 2006). Hybrids are two or more chemical entities with differing structural domains and biological activity, covalently linked together (Hulsman et al., 2007; Meunier, 2008). These distinct chemical entities should have independent pharmacophores (Meunier, 2008) and in addition, for the dual therapeutic action, should have distinct abilities to impart favourable physicochemical properties of one entity to another (Meunier, 2008; Walsh et al., 2007). The linker can be chosen carefully to allow the intact hybrid to dissociate into its individual components following administration (cleavable conjugates), whilst synergism in activity is aimed at, or to remain fixed when metabolically resistant linker units are chosen. The latter is the preferred option for overcoming resistance (Walsh and Bell, 2009).

Various artemisinin based hybrids have demonstrated promising biological activity and enhanced physicochemical properties, compared to the individual parent compounds (Capela et al., 2011; Lai et al., 2013; Muregi and Ishih, 2010; Njogu et al., 2013; Xie et al., 2011), but none has yet been approved from a regulatory perspective.

Acridine based compounds are the foundation of antimalarial drug research (Pérez et al., 2013). Indeed, mepacrine (Fig. 2), the first blood schizontocide, had been used as first line treatment of malaria during World War II, but was discontinued shortly thereafter, due to reported toxicity (Elueze et al., 1996). Acridines reportedly own their biological activity to various mechanisms of action, including DNA intercalators, inhibitors of mammalian topoisomerases I and II and acetylcholinesterase (Ciesielska et al., 1997; Valdés, 2011). Recently, various synthetic and semi-synthetic acridinone analogues have been synthesized. Screen tests of 3-(5,6,6,6-tetrafluoro-5-trifluoromethyl-hexyloxy)-6-chloroacridinone exhibited potent antimalarial activity, with a 50% inhibitory concentration (IC_{50}) value of 1 nM against the D6 sensitive strain of *P. falciparum*, as well as low cytotoxicity towards murine splenic lymphocytes (Winter et al., 2006). The quinacrine-floxacrine hybrid, WR 243251, exhibited nanomolar IC_{50} values of 11 nM against CQ sensitive D6, and 25 nM against CQ resistant W2 *P. falciparum* strains (Berman et al., 1994), with limited side effects (Biagini et al., 2008).

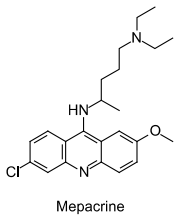

Fig. 2. Structure of mepacrine. Mepacrine was the first synthetic antimalarial drug but abandoned for toxicity reason.

In search for new antimalarial drugs and in light of the above considerations, hybrids, synthesized through the chemical combination of acridine and artemisinin pharmacophores with various linkers were investigated. In this paper, the synthesis, *in vitro* antimalarial activity cytotoxicity and apoptotic/anticancer activity are reported.

2. Materials and methods

2.1. Materials

Ethylenediamine, *N*-methyl-1,3-propylenediamine, piperazine, 2-methylpiperazine, 1-(2-aminoethyl)piperazine, 6,9-dichloro-2-methoxyacridine, magnesium sulphate ($MgSO_4$), sodium bicarbonate ($NaHCO_3$), potassium carbonate (K_2CO_3), acetonitrile (ACN), ammonium hydroxide solution (NH_4OH), *N*,*N*-dimethylformamide (DMF), tetrahydrofuran (THF), deuterated dimethyl sulfoxide (DMSO-d_6), deuterated chloroform ($CDCl_3$-*d*), boron trifluoride diethyl etherate (BF_3–Et_2O) and 2-bromoethanol were all purchased from Sigma–Aldrich (South-Africa). Potassium iodide (KI) was obtained from Merck (South-Africa). All solvents used were acquired from Associated Chemical Enterprises (ACE, South Africa). Dihydroartemisinin (mixture of 10-α and 10-β epimers) was purchased from Changzhou Kaixuan Chemical Co (Chunjiang, China). All chemicals, i.e. methanol (MeOH), dichloromethane (DCM), ethyl acetate (EtOAc) and reagents were of analytical grade and were used without further purification.

2.2. General procedures

The ^1H and ^{13}C NMR spectra were recorded on a Bruker Advance™ III 600 spectrometer at a frequency of 600 MHz and 150.913 MHz, respectively, in DMSO-d_6 or $CDCl_3$-*d*. Chemical shifts are reported in parts per million δ (ppm), with the residual protons of the solvent as reference. The splitting pattern abbreviations are as follows: singlet (s), doublet (d), doublet of doublet (dd), doublet of doublet of doublets (ddd), doublet of triplets (dt), doublet of quartets (dq), triplet (t), triplet of doublets (td), triplet of triplets (tt), quartet of doublets (qd), multiplet (m).

High resolution mass spectrometry (HRMS) was recorded on a Bruker MicroTOF Q II mass spectrometer, equipped with an APCI or an ESI source set at 200 °C or 180 °C, respectively, with Bruker Compass DataAnalysis 4.0 software. A full scan from 50 to 1500 m/z was generated, at a capillary voltage of 4500 V, an end plate offset voltage of −500 V, the nebulizer set at 1.6 and 0.4 bar, respectively and a collision cell RF voltage of 100 Vpp.

Infrared (IR) spectra were recorded on a Bruker Alpha-P FTIR instrument. Melting points (mp) were determined on a BÜCHI melting point B-545 instrument in triplicate and were uncorrected.

Thin layer chromatography was performed using silica gel plates ($60F_{254}$) obtained from Merck. Column chromatography was performed using MN silica gel 60, 70–230 mesh ASTM, supplied by Macerey–Nagel (Germany).

All microwave assisted reactions were carried out in a CEM Discovery™ microwave synthesizer focused closed vessel. The machine consisted of a continuously focused microwave power delivery system, selectable power output between 0 and 300 W, a maximum current of 6.3 amps and a frequency of 50/60 Hz. The temperature of the vessel's contents was continuously monitored *via* an IR sensor, located underneath the reaction vessel. The reaction mixture was stirred with a Teflon coated magnetic stir bar *via* a rotating magnetic plate, located below the microwave cavity floor.

2.3. Synthesis

2.3.1. 2-Bromo-(10β-dihydroartemisinoxy)ethane, **1**

2-Bromo-(10β-dihydroartemisinoxy)ethane **1** (Fig. 3) analogue of DHA was synthesized in moderate yields (71%) from DHA and 2-bromoethanol by using a reported method of Li et al. (2000), routinely used by our research group.

^{1}H NMR (600 MHz, $CDCl_3$) δ (ppm): 5.46 (s, 1H, H-12), 4.82 (d, *J* = 3.4 Hz, 1H, H-10), 4.13 (dt, *J* = 10.8, 5.4 Hz, 1H, H-aα), 3.76 (dt, *J* = 10.9, 5.3 Hz, 1H, H-aβ), 3.53 (t, 2H, H-b), 2.66 (dt, *J* = 7.7, 5.7 Hz, 1H, H-9), 2.33 (tt, *J* = 20.2, 10.0 Hz, 1H, H-4α), 2.04–1.97 (m, 1H, H-4β), 1.91–1.80 (m, 2H, H-8α, H-5α), 1.73 (ddd, *J* = 14.2, 7.5, 3.6 Hz, 1H, H-8β), 1.65–1.55 (m, 1H, H-7β), 1.52–1.37 (m, 5H, H-8a, H-5β, H-14), 1.36–1.28 (m, 1H, H-6), 1.25–1.17 (m, 1H, H-5a), 0.89 (m, 7H, H-7α, H-15, H-16); ^{13}C NMR (151 MHz, $CDCl_3$) δ (ppm): 104.10 (C-3), 102.02 (C-10), 88.12 (C-12), 81.02 (C-12a), 68.15 (C-a), 52.55 (C-5a), 44.33 (C-8a), 37.37 (C-6), 36.37 (C-4), 34.63 (C-7), 31.41 (C-b), 30.83 (C-9), 26.12 (C-14), 24.62 (C-5), 24.34(C-8), 20.31(C-15), 12.91 (C-16); APCI-HRMS *m/z* $[M+H]^+$: 392.1400 (Calcd. for $C_{21}H_{36}NO_6$: 391.1115).

2.3.2. 9-Aminoacridines, **2**–**6**

An adapted literature method of Ishikawa et al. (2001) served to synthesize the 9-aminoacridines. It is described as follows: 6,9-dichloro-2-methoxyacridine (7.1 mmol, 2.0 g, 1 eq.) was dissolved in anhydrous DMF (40 ml) upon stirring at 60–80 °C for 5–10 min and K_2CO_3 (7.2 mmol, 1.0 g, 1 eq.) added, followed by the appropriate amine, either di- or triamine (143.8 mmol, 20 eq.) (Scheme 1). The resulting mixture was stirred for an additional 3–6 h until completion of the reaction (Scheme 1). Thereafter, the reaction mixture was filtered and the filtrate was spun to dryness *in vacuo*. The residue was dissolved in DCM (50 ml) and the organic phase washed with saturated $NaHCO_3$ (3 × 50 ml), brine (50 ml) and water (50 ml), and dried over $MgSO_4$. The solvent was removed *in vacuo*, resulting in a yellow powder/oil, which was purified through column chromatography by successively eluting with various ratios of MeOH, DCM, EtOAc and NH_4OH.

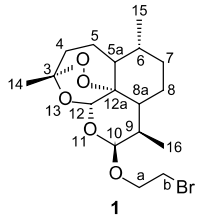

1

Fig. 3. The 2-bromo-(10β-dihydroartemisinoxy)ethane analogue of DHA. Compound **1** was synthesized from DHA and 2-bromoethanol using routinely methods.

*2.3.2.1. N-(2-aminoethyl)-6-chloro-2-methoxyacridin-9-amine, **2**.* The reaction of 6,9-dichloro-2-methoxyacridine and ethylenediamine, followed by successive purification through chromatography, eluting with DCM:MeOH:NH_4OH (8:1.5:0.5, v/v/v) then MeOH:NH_4OH (19:1, v/v) afforded **2** (1.6 g, 75%) a yellow–brown powder; mp: 164 °C; IR (ATR) ν_{max}/cm^{-1}: 3343, 1631, 1557, 750, 580; ^{1}H NMR (600 MHz, $CDCl_3$) δ (ppm): 8.06 (d, *J* = 9.1 Hz, 1H, H-8′), 8.01–7.95 (m, 1H, H-5′), 7.93 (d, *J* = 9.3 Hz, 1H, H-4′), 7.37 (dd, *J* = 9.4, 2.7 Hz, 1H, H-3′), 7.30 (d, *J* = 2.7 Hz, 1H, H-1′), 7.24–7.22 (m, 1H, H-7′), 5.90 (s, 1H, H-11′), 3.91 (s, 3H, H-10′), 3.63 (t, *J* = 5.5 Hz, 2H, H-12′), 2.94 (dd, *J* = 6.3, 4.8 Hz, 2H, H-13′); ^{13}C NMR (151 MHz, $CDCl_3$) δ (ppm): 155.84 (C-2′), 150.20 (C-9′), 148.38, 146.74, 134.62 (C-6′), 131.31 (C-4′), 128.08 (C-5′), 124.46 (C-8′), 124.24 (C-7′), 118.28, 116.16, 99.30 (C-1′), 55.43 (C-10′), 51.50 (C-12′), 41.92 (C-13′); APCI-HRMS *m/z* $[M+H]^+$: 302.1051 (calcd. for $C_{16}H_{17}ClN_3O$: 302.1054).

*2.3.2.2. {3-[(6-Chloro-2-methoxyacridin-9-yl)amino]propyl}(methyl) amine, **3**.* The reaction of 6,9-dichloro-2-methoxyacridine and *N*-methyl-1,3-diaminopropane, followed by successive purification through chromatography, eluting with DCM:MeOH:NH_4OH (8:1.5:0.5, v/v/v) then MeOH:NH_4OH (19:1, v/v) afforded **3** (1.9 g, 79%) an off-white to yellow powder; mp: 165 °C; IR (ATR) ν_{max}/cm^{-1}: 3374, 1633, 1563, 675, 560; ^{1}H NMR (600 MHz, DMSO-d_6) δ (ppm): 8.31 (d, *J* = 9.3 Hz, 1H, H-8′), 7.82 (d, *J* = 2.2 Hz, 1H, H-5′), 7.78 (d, *J* = 9.3 Hz, 1H, H-4′), 7.55 (d, *J* = 2.7 Hz, 1H, H-1′), 7.38 (dd, *J* = 9.2, 2.6 Hz, 1H, H-3′), 7.25 (dd, *J* = 9.3, 2.3 Hz, 1H, H-7′), 3.91 (s, 3H, H-10′), 3.86 (q, *J* = 5.9, 5.2 Hz, 2H, H-12′), 3.56–3.09 (m, 4H, H_2O), 2.61 (t, *J* = 6.1 Hz, 2H, H-14′), 2.49 (p, *J* = 1.8 Hz, 4H, H-16′), 2.26 (s, 2H, H-15′), 1.81 (p, *J* = 6.4 Hz, 2H, H-13′); ^{13}C NMR (151 MHz, DMSO-d_6) δ (ppm): 154.90 (C-2′), 150.25 (C-9′), 148.31, 133.32 (C-6′), 130.49 (C-4′), 126.78 (C-5′), 123.90 (C-8′), 122.07 (C-7′), 116.53, 113.95, 100.59 (C-1′), 55.50 (C-10′), 49.81 (C-12′), 48.88 (C-13′), 36.24 (C-16′), 29.57 (C-14′); APCI-HRMS *m/z* $[M+H]^+$: 330.1354 (Calcd. for $C_{18}H_{21}ClN_3O$: 330.1367).

*2.3.2.3. 6-Chloro-2-methoxy-9-(piperazin-1-yl)acridine, **4**.* The reaction of 6,9-dichloro-2-methoxyacridine and piperazin, followed by successive purification through chromatography, eluting with DCM:EtOAc (1:1, v/v) then MeOH:NH_4OH (19:1, v/v) afforded **4** (1.7 g, 73%) a yellow powder; mp: 163 °C; IR (ATR) ν_{max}/cm^{-1}: 3532, 3293, 1627, 766, 564; ^{1}H NMR (600 MHz, DMSO-d_6) δ (ppm): 8.39 (d, *J* = 9.2 Hz, 1H, H-8′), 8.08 (d, *J* = 2.2 Hz, 1H, H-5′), 7.99 (d, *J* = 9.3 Hz, 1H, H-4′), 7.53–7.49 (m, 3H, H-1′, H-3′, H-7′), 3.96 (s, 2H, H-10′), 3.49 (t, *J* = 4.6 Hz, 4H, H-12′, H-14′), 3.39 (s, 61H, H_2O), 3.05 (t, *J* = 4.6 Hz, 4H, H-13′, H-15′); ^{13}C NMR (151 MHz, DMSO-d_6) δ (ppm): 156.30 (C-2′), 152.54 (C-9′), 148.23, 147.41, 133.51 (C-6′), 131.42 (C-4′), 127.87 (C-5′), 126.81 (C-8′), 125.55 (C-7′), 125.24 (C-3′), 124.57, 122.28, 100.68 (C-1′), 55.51 (C-10′), 52.83 (C-12′, C-14′), 46.64 (C-13′, C-15′); APCI-HRMS *m/z* $[M+H]^+$: 328.1200 (Calcd. for $C_{18}H_{19}ClN_3O$: 328.1211).

*2.3.2.4. 6-Chloro-2-methoxy-9-(3-methylpiperazin-1-yl)acridine, **5**.* The reaction of 6,9-dichloro-2-methoxyacridine and 2-methylpiperazin, followed by successive purification through chromatography, eluting with DCM:MeOH:NH_4OH (8:1.5:0.5, v/v/v) then MeOH:NH_4OH (19:1, v/v) afforded **5** (1.2 g, 45%) a yellow–reddish powder; mp: 165 °C; IR (ATR) ν_{max}/cm^{-1}: 3275, 1628, 1417, 169, 652; ^{1}H NMR (600 MHz, $CDCl_3$) δ (ppm): 8.36 (d, *J* = 9.2 Hz, 1H, H-8′), 8.07 (s, 1H, H-5′), 7.98 (d, *J* = 9.3 Hz, 1H, H-4′), 7.57–7.49 (m, 3H, H-1′, H-3′, H-7′), 3.95 (s, 3H, H-10′), 3.36 (s, 46H, H_2O, H-14′, H-13′, H-15′), 3.09–3.04

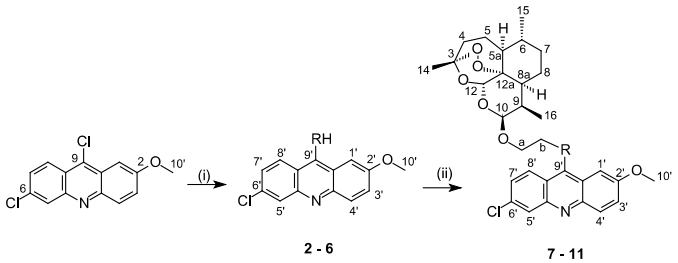

Compound	R	Compound	R
2	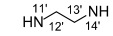	7	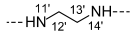
3	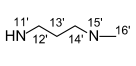	8	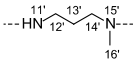
4		9	
5		10	
6	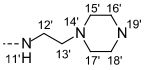	11	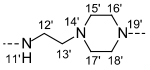

Scheme 1. Multi-step synthesis of artemisinin–acridine hybrids **7**–**11**. Reagents and conditions: (i) appropriate amine, DMF, 3–6 h, 60–80 °C and (ii) **1**, **2**–**7**, ACN, KI, K_2CO_3, microwave (150 W, 45 °C).

(m, 2H, H-12′), 1.03 (d, *J* = 6.1 Hz, 2H, H-17′); ^{13}C NMR (151 MHz, $CDCl_3$) δ (ppm): 156.93 (C-2′), 152.49 (C-9′), 148.67, 148.01, 133.43 (C-6′), 131.38 (C-4′), 127.87 (C-5′), 126.84 (C-8′), 125.41 (C-7′), 125.15 (C-3′), 124.47, 122.17, 100.70 (C-1′) 59.78 (C-14′), 55.45 (C-10′), 52.48 (C-12′), 51.54 (C-13′), 46.76 (C-15′), 19.12 (C-17′); APCI-HRMS *m*/*z* $[M + H]^+$: 342.1364 (Calcd. for $C_{19}H_{20}ClN_3O$: 342.1367).

2.3.2.5. 6-Chloro-2-methoxy-N-[2-(piperazin-1-yl)ethyl]acridin-9-amine, ***6****.* The reaction of 6,9-dichloro-2-methoxyacridine and 1-(2-aminoethyl)piperazine, followed by successive purification through chromatography, eluting with DCM:MeOH:NH_4OH (8:1.5:0.5, v/v/v) then MeOH:NH_4OH (19:1, v/v) resulted in **6** (1.0 g, 45%) an off-white to yellow powder; mp: 166 °C; IR (ATR) ν_{max}/cm^{-1}: 3407, 3332, 2819, 1631, 557; ^{1}H NMR (600 MHz, $CDCl_3$) δ (ppm): 8.12 (d, *J* = 9.2 Hz, 1H, H-8′), 8.07–8.05 (m, 1H, H-5′), 8.01–798 (d, *J* = 9.4 Hz, 1H, H-4′), 7.42 (dd, *J* = 9.4, 2.7 Hz, 1H, H-3′), 7.27 (tt, *J* = 4.7, 2.4 Hz, 2H, H-1′, H-7′), 6.24 (s, 1H, H-11′), 3.98 (s, 3H, H-10′), 3.80 (t, *J* = 5.7 Hz, 2H, H-12′), 3.00 (t, *J* = 4.9 Hz, 4H, H-16′, H-18′), 2.67 (t, *J* = 5.7 Hz, 2H, H-15′), 2.68–2.56 (m, 4H, H-13′, H-17′); ^{13}C NMR (151 MHz, $CDCl_3$) δ (ppm): 155.76 (C-2′), 150.15 (C-9′), 148.41, 146.51, 134.70 (C-6′), 131.27 (C-4′), 127.99 (C-5′), 124.50 (C-8′), 124.42 (C-7′), 124.26 (C-3′), 123.98 117.51, 115.41, 99.10 (C-1′), 57.88 (C-13′), 55.46 (C-10′), 55.42, 53.87 (C-15′, C-17′), 46.94 (C-16′), 46.33 (C-18′), 45.62 (C-12′); APCI-HRMS *m*/*z* $[M + H]^+$: 371.1619 (Calcd. for $C_{20}H_{24}ClN_4O$: 371.1633).

2.3.3. Artemisinin–acridine hybrids, 6–11

9-Aminoacridine, **2–6** (1 eq.) and **1** (1.5 eq.) were dissolved in ACN (40 ml) at room temperature, and $NaHCO_3$ (1 eq.) and KI (catalytic amount) were added. The reaction mixture was transferred into a 100 ml round-bottomed flask and placed in a CEM Discovery™ microwave synthesizer explorer carousel (Scheme 1). The mixture was heated to 45 °C while stirring for 10 min (150 W, 50 psi), then left to cool for 10 min at room temperature. This procedure was repeated, until completion of the reaction. Afterwards, the mixture was filtered and the filtrate spun to dryness, leaving a yellow residue, which was dissolved in DCM. The organic phase was washed with $NaHCO_3$ (3 × 50 ml), brine (50 ml) and water (50 ml) and dried over $MgSO_4$. The solvent was removed *in vacuo* and the residue purified through column chromatography, eluting with various ratios of MeOH, DCM, EtOAc and NH_4OH to afford the target hybrids. The IR, NMR and HRMS data are reported below.

2.3.3.1. {N-(2-aminoethyl)-6-chloro-2-methoxyacridin-9-amine}-2-(10β-dihydroartemisinoxy)ethane, ***7****.* The reaction of **1** (5.0 mmol, 1.9 g), **2** (3.3 mmol, 1.0 g) and K_2CO_3 (5.0 mmol, 0.7 g), followed by purification on silica gel, eluting with DCM:MeOH;NH_4OH (9:0.5:0.5, v/v/v) afforded **7** (0.2 g, 7%) yellow–brown crystals; mp: 166 °C; IR (ATR) ν_{max}/cm^{-1}: 3310, 2920, 1630, 1012, 563; ^{1}H NMR (600 MHz, $CDCl_3$) δ (ppm): 8.07 (dd, *J* = 15.0, 9.3 Hz, 1H, H-8′), 7.93 (d, *J* = 2.1 Hz, 1H, H-5′), 7.88 (d, *J* = 9.3 Hz, 1H, H-4′), 7.32 (d, *J* = 2.7 Hz, 1H, H-1′), 7.16 (dd, *J* = 9.2, 2.4 Hz, 1H, H-3′), 7.07 (dd, *J* = 9.1, 2.1 Hz, 1H, H-7′), 5.37 (s, 1H, H-12), 4.82 (d,

J = 3.5 Hz, 1H, H-10), 4.27–4.11 (m, 2H, H-13′), 4.05 (dt, *J* = 10.4, 5.2 Hz, 1H, H-aα), 3.94 (s, 4H, H-10′), 3.89–3.72 (m, 1H), 3.64 (ddd, *J* = 14.3, 10.0, 5.5 Hz, 1H, H-aβ), 3.31 (dh, *J* = 12.2, 6.7 Hz, 2H, H-12′), 3.03 (t, *J* = 5.4 Hz, 2H, H-b), 2.62 (qt, *J* = 7.5, 3.9 Hz, 1H, H-9), 2.44–2.23 (m, 2H, H-4α), 2.14 (s, 1H), 2.06–1.91 (m, 2H, H-4β), 1.92–1.53 (m, 5H, H-5, H-8α), 1.50–1.15 (m, 15H, H-8β, H-8a, H-14, H-7, H-6, H-5a), 0.93–0.70 (m, 15H, H-16, H-15); ^{13}C NMR (151 MHz, $CDCl_3$) δ (ppm): 158.18, 156.15 (C-2′), 152.68 (C-9′), 139.30, 134.95 (C-6′), 131.85 (C-4′), 128.70 (C-5′), 126.28 (C-8′), 125.92 (C-7′), 125.69 (C-3′), 124.10, 122.91, 104.13 (C-3), 102.35 (C-10), 101.23 (C-1′), 98.45, 87.96, 87.88 (C-12), 80.93 (C-12a), 67.73 (C-a), 66.83, 55.92(C-10′), 55.60, 53.40, 52.48, 52.38 (C-5a), 48.49 (C-b), 47.77 (C-12′), 47.06 (C-13′), 46.08, 44.69, 44.22 (C-8a), 37.41 (C-6), 36.32 (C-4), 34.47 (C-7), 31.90, 30.79 (C-9), 29.67, 29.34, 26.15, 26.10 (C-14), 24.60 (C-8), 24.56 (C-5), 22.67, 20.22 (C-15), 14.10, 13.06 (C-16); ESI-HRMS *m*/*z* $[M+H]^+$: 612.2825 (Calcd. for $C_{33}H_{43}ClN_3O_6$: 612.2835).

2.3.3.2. {3-[(6-Chloro-2-methoxyacridin-9-yl)amino]propyl}(methyl) amine-2-(10β-dihydroartemisinoxy)ethane, ***8***. The reaction between **1** (4.6 mmol, 1.8 g), **3** (3 mmol, 1.0 g) and K_2CO_3 (5.0 mmol, 0.7 g), followed by purification on silica gel, eluting with DCM:MeOH;NH_4OH (9:0.5:0.5, v/v/v) afforded **8** (1.1 g, 59%) yellow crystals; mp: 171 °C; IR (ATR) ν_{max}/cm^{-1}: 3309, 2920, 1630, 1023, 665; ^{1}H NMR (600 MHz, $CDCl_3$) δ (ppm): 8.03 (d, *J* = 2.1 Hz, 1H, H-5′), 8.00 (dd, *J* = 9.3, 4.6 Hz, 2H, H-8′, H-4′), 7.33 (dd, *J* = 9.3, 2.6 Hz, 1H, H-3′), 7.28 (d, *J* = 2.6 Hz, 1H, H-1′), 7.17 (dd, *J* = 9.2, 2.1 Hz, 1H, H-7′), 5.33 (s, 1H, H-12), 4.77 (d, *J* = 3.7 Hz, 1H, H-10), 4.08–4.03 (m, 3H, H-13′, H-aα), 3.92 (s, 3H, H-10′), 3.61 (ddd, *J* = 10.9, 6.4, 4.4 Hz, 1H, H-aβ), 2.79 (dddd, *J* = 10.9, 6.5, 4.4, 1.9 Hz, 2H, H-b), 2.71 (dddd, *J* = 19.1, 12.8, 6.6, 4.2 Hz, 2H), 2.55 (dp, *J* = 11.5, 4.3, 3.8 Hz, 1H, H-9), 2.42 (s, 3H, H-16′), 2.26 (td, *J* = 14.0, 3.9 Hz, 1H, H-4α), 1.90 (dtd, *J* = 12.9, 7.6, 6.2, 3.8 Hz, 3H, H-4β), 1.69 (ddt, *J* = 13.6, 6.7, 3.5 Hz, 1H, H-8α), 1.58 (qd, *J* = 13.7, 3.5 Hz, 1H, H-5α), 1.49 (dq, *J* = 14.1, 3.8 Hz, 1H, H-8β), 1.37 (s, 3H, H-14′), 1.31 (dt, *J* = 13.5, 4.6 Hz, 1H, H-6), 1.25–1.13 (m, 2H), 1.07–1.05 (m, 2H, 5a), 0.98–0.73 (m, 5H, H-7α, H-16), 0.63–0.61 (m, 4H, H-7β, H-15); ^{13}C NMR (151 MHz, $CDCl_3$) δ (ppm): 155.22 (C-2′), 151.72 (C-9′), 125.07 (C-8′), 123.83 (C-7′), 123.30 (C-3′), 115.86, 113.35, 104.06 (C-3), 102.59 (C-10), 101.75 (C-1′), 87.91 (C-12), 80.92 (C-12a), 66.42 (C-a), 58.25 (C-b), 57.34 (C-13′), 55.66 (C-10′), 52.25 (C-5a), 51.32 (C-12′), 44.12 (C-8a), 43.31 (C-16′), 37.22 (C-6), 36.29 (C-4), 34.30 (C-7), 30.71 (C-9), 26.62, 26.11 (C-14), 24.47 (C-8), 24.34 (C-5), 20.03 (C-15), 12.92 (C-16); ESI-HRMS *m*/*z* $[M+H]^+$: 640.3134 (Calcd. for $C_{35}H_{47}ClN_3O_6$: 640.3148).

2.3.3.3. 6-Chloro-2-methoxy-9-(piperazin-1-yl)acridine-2-(10β-dihydroartemisinoxy)ethane, ***9***. The reaction between **1** (1.8 mmol, 0.7 g), **4** (1.2 mmol, 0.4 g) and K_2CO_3 (1.8 mmol, 0.3 g), followed by purification on silica gel, eluting with DCM:MeOH;NH_4OH (9:0.5:0.5, v/v/v) afforded **9** (1.2 g, 64%) yellow crystals; mp: 164.2 °C; IR (ATR) ν_{max}/cm^{-1}: 3466, 2953, 1629, 1015, 772; ^{1}H NMR (600 MHz, $CDCl_3$) δ (ppm): 8.25 (d, *J* = 9.2 Hz, 1H, H-8′), 8.17 (d, *J* = 2.1 Hz, 1H, H-5′), 8.08 (d, *J* = 9.3 Hz, 1H, H-4′), 7.49 (d, *J* = 2.8 Hz, 1H, H-1′), 7.43 (dd, *J* = 9.3, 2.7 Hz, 1H, H-3′), 7.36 (dd, *J* = 9.2, 2.2 Hz, 1H, H-7′), 5.52 (s, 1H, H-12), 4.86 (d, *J* = 3.4 Hz, 1H, H-10), 4.09–4.08 (m, 1H, H-aα), 3.98 (s, 3H, H-10′), 3.72–3.64 (m, 5H, H-aβ, H-12′, H14′), 2.87 (t, *J* = 37.4 Hz, 6H, H13′, H-15′ H-b), 2.65 (qt, *J* = 7.4, 4.1 Hz, 1H, H-9), 2.43–2.26 (m, 1H, H-4α), 2.04–2.02 (m, 1H, H-4β), 1.90–1.76 (m, 2H, H-8), 1.75 (dq, *J* = 14.3, 3.8 Hz, 1H, H-5α), 1.63 (dq, *J* = 13.2, 3.4 Hz, 1H, H-5β), 1.48 (ddt, *J* = 21.9, 13.4, 4.7 Hz, 2H), 1.42 (s, 3H, H-14), 1.37 (dddd, *J* = 16.1, 12.5, 6.5, 3.8 Hz, 1H, H-6), 1.27–1.22 (m, 2H, H-5a), 0.94 (dd, *J* = 12.3, 6.8 Hz, 6H, H-15, H-16), 0.90–0.78 (m, 1H); ^{13}C NMR (151 MHz, $CDCl_3$) δ (ppm): 156.93 (C-2′), 134.91 (C-6′), 131.15 (C-4′), 128.01 (C-5′), 126.17 (C-8′), 125.64 (C-7′), 125.48 (C-3′), 122.84, 104.12 (C-3), 102.07 (C-10), 100.40 (C-1′), 87.97 (C-12), 81.05 (C-12a), 65.54 (C-a), 60.37 (C-13′, C-15′), 58.20 (C-b), 55.72 (C-10′), 55.72, 54.71, 52.51 (C-5a), 51.93, 51.85, 44.34 (C-8a), 37.61 (C-6), 36.39 (C-4), 34.65 (C-7), 30.80 (C-9), 26.16 (C-14), 24.74 (C-8), 24.45 (C-5), 20.38 (C-15), 13.10 (C-16); APCI-HRMS *m*/*z* $[M+H]^+$: 638.3005 (Calcd. for $C_{35}H_{45}ClN_3O_6$: 638.2991).

2.3.3.4. 6-Chloro-2-methoxy-9-(2-methylpiperazin-1-yl)acridine-2-(10β-dihydroarte misinoxy)ethane, ***10***. The reaction between **1** (4.4 mmol, 1.7 g), **5** (2.9 mmol, 1.0 g) and K_2CO_3 (4.40 mmol, 0.6 g), followed by purification on silica gel, eluting with DCM:MeOH;NH_4OH (9:0.5:0.5, v/v/v) afforded **10** (0.5 g, 64%) yellow crystals; mp: 168 °C; IR (ATR) ν_{max}/cm^{-1}: 3419, 2919, 1629, 1024, 568; ^{1}H NMR (600 MHz, $CDCl_3$) δ (ppm): 8.26 (d, *J* = 9.3 Hz, 1H, H-8′), 8.16–8.15 (m, 1H, H-5′), 8.07 (d, *J* = 9.5 Hz, 1H, H-4′), 7.50 (t, *J* = 3.7 Hz, 1H, H-1′), 7.42 (dd, *J* = 9.3, 2.7 Hz, 1H, H-3′), 7.36 (ddd, *J* = 10.9, 5.2, 2.2 Hz, 1H, H-7′), 5.54 (d, *J* = 30.9 Hz, 1H, H-12), 4.86 (dd, *J* = 7.2, 3.5 Hz, 2H, H-10), 4.08 (q, *J* = 17.1, 13.4 Hz, 1H, H-aα), 3.97 (d, *J* = 2.6 Hz, 3H, H-10′), 3.74–3.59 (m, 1H, H-aβ), 3.55–3.33 (m, 2H, H-12′, H-14′), 3.19 (d, *J* = 36.3 Hz, 1H, H-13′), 2.89 (d, *J* = 75.2 Hz, 1H, H-15′), 2.67–2.65 (m, 1H, H-9), 2.37 (tt, *J* = 14.0, 4.5 Hz, 1H, H-4α), 2.04 (ddt, *J* = 14.8, 4.9, 2.3 Hz, 1H, H-4β), 1.90–1.73 (m, 3H, H-8), 1.61 (ddq, *J* = 12.9, 6.7, 3.5 Hz, 1H, H-5β), 1.43 (d, *J* = 1.5 Hz, 3H, H-14), 1.23 (dtt, *J* = 13.4, 6.9, 4.0 Hz, 4H, H-17′, H-6), 0.96–0.90 (m, 7H, H-7β, H-16, H-15); ^{13}C NMR (151 MHz, $CDCl_3$) δ (ppm): 159.79, 157.18, 156.91 (C-2′), 148.64 (C-9′), 135.22 (C-6′), 131.38, 131.25 (C-4′), 128.28, 128.27 (C-5′), 128.15, 126.67, 126.12, 125.39, 125.20, 123.39, 120.92, 118.70, 104.13 (C-3), 102.36 (C-10), 100.37, 97.42 (C-1′), 87.99 (C-12), 87.95, 81.05 (C-12a), 81.03, 70.52, 63.34 (C-a), 55.67 (C-10′), 52.63 (C-12′, C-14′), 52.50 (C-5a), 44.31 (C-8a), 37.60, 37.57 (C-6), 36.40 (C-4), 36.38, 34.60 (C-7), 30.81, (C-9), 26.16 (C-14), 24.77 (C-8), 24.70 (C-5), 24.45, 20.36 (C-16), 13.16 (C-15), 13.09 (C-17′); ESI-HRMS *m*/*z* $[M+H]^+$: 652.3142 (Calcd. for $C_{36}H_{47}ClN_3O_6$: 652.3148).

2.3.3.5. 6-Chloro-2-methoxy-N-[2-(piperazin-1-yl)ethyl]acridin-9-amine-2-(10β-dihydroartemisinoxy)ethane, ***11***. The reaction between **1** (4.1 mmol, 1.6 g), **6** (2.7 mmol, 1.0 g) and K_2CO_3 (4.1 mmol, 0.6 g), followed by purification on silica gel, eluting with DCM:MeOH;NH_4OH (9:0.5:0.5, v/v/v) afforded **11** (1.3 g, 71%) yellow crystals; mp: 168 °C; IR (ATR) ν_{max}/cm^{-1}: 3334, 2937, 1630, 1022, 563; ^{1}H NMR (600 MHz, $CDCl_3$) δ (ppm):): 8.07 (d, *J* = 9.2 Hz, 1H, H-8′), 8.03 (d, *J* = 2.0 Hz, 1H, H-5′), 7.98 (d, *J* = 9.4 Hz, 1H, H-4′), 7.32 (d, *J* = 2.6 Hz, 1H, H-3′), 7.22 (d, *J* = 2.6 Hz, 1H, H-1′), 7.20 (d, *J* = 2.2 Hz, 1H, H-7′), 5.45 (s, 1H, H-12), 4.80 (d, *J* = 3.5 Hz, 1H, H-10), 3.95 (s, 5H, H-13′, H-10′), 3.88 (t, *J* = 6.4 Hz, 3H, H-aα H-12′), 3.55 (dt, *J* = 10.9, 5.8 Hz, 1H, H-aβ), 2.73 (t, *J* = 5.7 Hz, 2H, H-b, H-9), 2.34 (td, *J* = 14.0, 3.9 Hz, 1H, H-4α), 2.00 (ddd, *J* = 14.6, 4.9, 3.0 Hz, 1H, H-4β), 1.86–1.72 (m, 3H, H-8), 1.71 (dq, *J* = 14.2, 3.9 Hz, 1H, H-5α), 1.58 (dq, *J* = 12.9, 3.3 Hz, 1H, H-5β), 1.46–1.37 (m, 6H, H-14), 1.36–1.32 (m, 1H, H-6), 1.23–1.20 (m, 2H, H-5a), 0.92–0.86 (m, 9H, H-15, H-16, H-7); ^{13}C NMR (151 MHz, $CDCl_3$) δ (ppm): 155.90 (C-2′), 150.89 (C-9′), 124.98 (C-7′), 124.86 (C-3′), 124.05 (C-8′), 104.03 (C-3), 101.97 (C-10), 99.54 (C-1′), 87.92 (C-12), 81.09 (C-12a), 65.92 (C-a), 57.92 (C-b), 56.90 (C-16′, C-18′), 55.61 (C-10′), 53.80 (C-15′, C-17′), 52.65, 52.52 (C-5a), 45.40 (C-12′), 44.38 (C-8a), 37.50 (C-6), 36.39 (C-4), 34.64 (C-7), 30.82 (C-9), 26.17 (C-14), 24.70 (C-8), 24.37 (C-5), 20.32 (C-15), 13.05 (C-16); ESI-HRMS *m*/*z* $[M+H]^+$: 681.3403 (Calcd. for $C_{37}H_{50}ClN_4O_6$: 681.3413).

Table 1
TGA and DSC data of compounds 7–11 and DHA. DSC served to determine the both the physical state and transition phases while TGA was used to determine the thermal stability.

Compd.	T1 (°C)[a,b]	T2 (°C)[a,b]	% weight loss-T2 [a]	Peak (°C)[b]	Peak onset (°C)[b]	Peak endset (°C)[b]	Heat loss (mJ)[b]
7	25	240	13.6	60.5	54.1	66.4	22.6
8	25	240	10.7	*	*	*	*
9	25	240	8.9	*	*	*	*
10	25	240	8.9	58.3	53.2	64.0	12.9
11	25	240	9.2	61.9; 96.7	58.5; 102.6	64.7; 98.4	23.1; 3.5
DHA	25	240	86.9	*	*	*	*

* = No data.
[a] TGA data determined by a Shimadzu DTG-60 and data interpreted by Schimadzu software).
[b] DSC data determined by a Shimadzu DSC-60 A and data interpreted by Schimadzu software.

2.4. Physicochemical properties

Differential scanning calorimetry (DSC) was performed, using a Shimadzu DSC-60, a LABCON low temperature water bath and a computer system. Data was collected for 2–4 mg samples weighed into aluminium crimp cells, covered and sealed with a crimping tool from Shimadzu. The samples were placed onto the auto sampler. This process was repeated with a reference that was placed manually on the left side of the furnace of the DSC apparatus. The DSC system parameters were set with a starting temperature of 25 °C, a maximum temperature of 300 °C, a heating rate of 10 °C/min and the nitrogen gas flow rate at 35 ml/min. The thermal process was started after the DSC trace was produced and analyzed, using the Schimadzu software. The results are reported in Table 1.

Thermogravimetric analysis (TGA) was performed by means of a Shimadzu DTG-60 and its computer system. Two empty aluminium crimp cells were placed on the furnace of the TGA and manually set to tear the microbalance. Data was collected for that quantity of sample that was placed in an aluminium cell and placed on the right hand side of the furnace, after which the system was closed. The system parameters were set with the starting temperature of 25 °C, a maximum temperature of 300 °C, a heating rate of 10 °C/min and the nitrogen gas flow rate at 35 ml/min. The sample was weighed automatically before starting the thermal process. A TGA trace was generated and analyzed, using the Schimadzu software. The results are reported in Table 1.

Accelrys Discovery Studio 3.1 was used to calculate the absorption, distribution, metabolism, and excretion – toxicity (ADMET) properties, including log*P*, aqueous solubility, human intestine absorption and blood brain barrier (BBB) levels of compounds **2–11**, and the results are summarized in Table 2.

Table 2
Predicted physicochemical parameters of compounds **2–11** (Accelrys Discovery Studio 3.1 served to calculate the predicted values).

Compound	Log*P*[a]	pK_a[b]	ADMET Solubility level[c]	ADMET Absorption level[d]	ADMET BBB level[e]
2	2.98	9.13	2	0	2
3	3.48	9.90	2	0	1
4	3.58	9.37	2	0	1
5	3.96	9.37	1	0	1
6	3.37	9.40	2	0	1
7	6.40	8.45	0	2	4
8	7.00	9.03	1	3	4
9	7.11	9.37	0	3	4
10	7.49	9.37	0	3	4
11	6.90	7.23	1	2	4

[a] Calculated using Accelrys Discovery Studio 3.1.
[b] Calculated using ACD.
[c] ADMET aqueous solubility level (LogS_w) at 25 °C and pH = 7, values = 0, 1, 2 and 3 indicate extremely low, very low, low and good solubility, respectively.
[d] ADMET human intestinal absorption, values = 0, 1, 2 and 3 indicate good, moderate, low and very low absorption, respectively.
[e] Blood brain barrier values = 0, 1, 2, 3, and 4 indicating, very high, high, medium, low and undefined blood–brain barrier penetration, respectively.

2.5. In vitro biological evaluation

2.5.1. Antimalarial activity

The test samples were screened in triplicate for the *in vitro* antiplasmodial activity determinations against a chloroquine sensitive (CQS) strain of *P. falciparum* (NF54) and against the chloroquine resistant (CQR) strain of *P. falciparum* (Dd2). Continuous *in vitro* cultures of asexual erythrocyte stages of *P. falciparum* were maintained, using a modified method of Trager and Jensen (1976). Quantitative assessment of antiplasmodial activity *in vitro* was determined by means of the parasite lactate dehydrogenase assay, using a modified method as described by Makler et al. (1993).

The test samples were prepared as 20 mg/ml stock solutions in 100% DMSO and were stored at −20 °C. Further dilutions were prepared in complete medium on the day of the experiment. Samples were tested as a suspension if not completely dissolved. Dihydroartemisinin (DHA), artesunate (AS) and chloroquine (CQ) were used as reference drugs. A full dose response analysis was performed to determine the IC_{50}-values. Test samples were tested at a starting concentration of 100 μg/ml, which was then serially diluted two-fold in complete medium to give ten concentrations per compound, with the lowest concentration being 0.2 μg/ml. The same dilution technique was used for all samples. References were tested at a starting concentration of 1000 ng/ml. The highest concentration of solvent to which the parasites were exposed to had no measurable effect on the parasites' viability (data not shown). The IC_{50} values were obtained using a non-linear, dose response, curve fitting analysis *via* Graph Pad Prism v.4.0 software. The results are reported in Table 3.

2.5.2. Cytotoxicity and anticancer activity

Test samples were screened for cytotoxicity and anticancer activity against the Chinese hamster ovarian (CHO) and HeLa cell lines, respectively, using the 3-(4,5-dimethylthiazol-2-yl)-2,5-diphenyltetrazoliumbromide (MTT) assay. The MTT assay is used as a colorimetric assay for the determination of cellular growth and survival, and compares well with other available assays (Mosmann, 1983; Rubinstein et al., 1990). The tetrazolium salt MTT was used to measure all growth and chemosensitivity. The test samples were tested in triplicate. The same stock solutions prepared for antiplasmodial testing were used for cytotoxicity testing. Test compounds were stored at −20 °C, until use. Dilutions were prepared on the day of the experiment. Emetine was used as the reference drug in all experiments. The initial concentration of emetine was 100 μg/ml, which was serially diluted in complete medium with ten-fold dilutions to give six concentrations per compound, the lowest being 0.001 μg/ml. The same dilution technique

Table 3
In vitro biological activity of compounds. Cells were incubated with compounds at various concentrations for 48 h; antimalarial activity and cytotoxicity against CHO and HeLa cells were determined using parasite lactate dehydrogenase (pLDH) and MTT-assays, respectively. Apoptosis against HepG2 and SH-SY5Y was determined using FITC annexin V/dead cell apoptosis assay.

Compound	Antimal. activity, IC_{50} (nM) ±S.D.[a]		Resistance index[b]	Cytotoxicity IC_{50} (μM) ±S.D.[c]	Antic. activity IC_{50} (μM) ±S.D.[c]	Apoptosis EC50 (μM) ±S.D.[d]		Selectivity index[e]
	NF54	Dd2	RI	CHO	HeLa	HepG2	SH-SY5Y	SI
2	13.9 ± 2.3	80.7 ± 8.3	5.8	1.0 ± 0.1	9.2 ± 1.2	55.2 ± 1.1	43.8 ± 1.1	72
3	9.1 ± 0.9	116.7 ± 15.8	12.8	0.5 ± 0	2.2 ± 1.3	47.4 ± 1.1	36.0 ± 1.2	55
4	1491.8 ± 68.8	1672.2 ± 152.2	1.1	3.4 ± 0	12.3 ± 1.1	56.8 ± 1.1	55.7 ± 1.1	2
5	158.3 ± 7.9	384.0 ± 45	2.4	5.6 ± 0	3.3 ± 1.2	15.1 ± 1.2	24.6 ± 1.2	35
6	7.3 ± 1.4	141.8 ± 4.1	19.4	0.3 ± 0.1	0.4 ± 1.3	58.7 ± 1.4	42.4 ± 1.1	41
7	2.6 ± 0.0	35.3 ± 3.6	13.6	1.6 ± 0.2	5.2 ± 1.4	55.1 ± 1.1	50.3 ± 1.2	615
8	12.2 ± 1.6	38.5 ± 1.6	3.2	1.2 ± 0.3	4.7 ± 1.3	54.6 ± 1.1	48.8 ± 1.1	98
9	266.8 ± 122.4	429.9 ± 10.2	1.6	>156.9	2.7 ± 1.8	33.6 ± 1.2	26.9 ± 1.1	>588
10	17.0 ± 2.1	41.3 ± 5.8	2.4	6.0 ± 1.1	3.3 ± nd[j]	55.6 ± 1.1	58.1 ± 1.1	353
11	14.1 ± 7.5	50.4 ± 2.9	3.6	0.9 ± 0.2	0.8 ± 2.5	58.2 ± 1.2	45.8 ± 1.1	64
DHA[f]	<7	7 ± 2	<1	20.1 ± 6.4	0.6 ± 1.3	44.3 ± 1.1	39.0 ± 1.1	>2871
AS[g]	<5.2	15.1 ± 0.5	<2.9	1.6 ± 0.5	0.5 ± 1.3	58.0 ± 1.1	57.1 ± 1.1	>308
CQ[h]	18.5 ± 6.3	271.7 ± 104.4	14.7	>312.6	17.7 ± 1.3	58.2 ± 1.2	58.1 ± 1.2	>16,897
EM[i]	nd	nd	nd	0.1			nd	nd
Melphalan					40 ± 2.3[k]			

[a,c] Antimalarial activity/cytotoxicity/apoptotic activity, IC_{50} value is the minimum concentration causing 50% cells growth inhibition, data represents the mean of three independent experiments SD (standard deviation).
[b] Resistance index (RI) = IC_{50}Dd2/IC_{50}NF54.
[d] Effective concentration of compound inducing 50% reduction in parasitic cells count, data represents the mean of three independent experiments SD (standard deviation), significance was set at $p \leqslant 0.05$.
[e] Selectivity index (SI) = IC_{50}CHO /IC_{50}NF54.
[f] Dihydroartemisinin (DHA).
[g] Artesunate (AS).
[h] Chloroquine (CQ) was tested as diphosphate salt.
[i] Emetine (EM) was used as the reference drug in the cytotoxicity study against CHO cells.
[j] Not determined (nd).
[k] IC_{50} value as reported by Ibrahim et al. (2013).

was applied to all test samples. The highest concentration of solvent to which the cells were exposed to had no measurable effect on the cell viability (data not shown). The IC_{50} values were obtained from full dose response curves, using a non-linear, dose response, curve fitting analysis *via* GraphPad Prism.

2.5.3. Apoptosis

Human hepatocellular cells (HepG2) and human neuroblastoma cells (SH-SY5Y) were used for the apoptosis assay. Dilutions of the compounds were prepared on the day of the experiment. The initial concentration of 200 μM was serially diluted in complete medium with two-fold dilutions to give eight concentrations per compound, the lowest being 0.01 μM. The same dilution technique was applied to all test samples. The highest concentration of solvent to which the cells were exposed to had no measurable effect on the cell viability (data not shown). An FITC annexin V/dead cell apoptosis kit, equipped with FITC annexin V and PI for flow cytometry were used to simultaneously determine the numbers of live, dead and apoptotic cells.

Apoptosis was induced for 4 h in the cells through the addition of 1 ml of the stock solution (1 mM). A negative control was prepared simultaneously, without the inducing agent and the positive control was staurosporine (500 nM). The cells were harvested and washed in 100 ml cold phosphate buffered saline (PBS) solution, while the required annexin binding buffer was prepared. A 100 μg/ml PI solution was prepared by diluting 100 μl of the 1 mg/ml PI stock solution in 45 μL of 1× annexin binding buffer. After the washed cells had been re-centrifuged and the resulting supernatant removed, the cells were re-suspended in 1× annexin binding buffer. The cell density was determined and adjusted where needed to the required concentration of $\sim 1 \times 10^6$ cells/ml. To each 100 μl of cell suspension, 5 μl of FITC annexin V and 1 μl of the 100 μg/ml PI were added. The cells were incubated for 15–20 min at room temperature and protected from light. Thereafter, 400 μl of 1× annexin binding buffer was gently mixed into the cells and kept on ice. After incubation, the stained cells underwent quantitative assessment through flow cytometry, quantifying fluorescence excitation/emission wavelengths at 530 nm and >575 nm. The cells were detected in three separate groups, i.e. live cells with a low level of green fluorescence, apoptotic cells with green fluorescence and dead cells with red and green fluorescence.

The data was processed with FCS Express v.4 software. Gates were set on the dot plot FSC and SSC during analysis. The geometric means of fluorescence for all of the parameters were calculated from the respective histograms, or from two parameter fluorescence dot plots. The results are expressed in arbitrary units as mean fluorescence intensity (MFI). The statistical significance was determined with one way analysis of variance (ANOVA) with Dunn's multiple comparison tests for non-parametric statistics. The data is presented as mean ± standard deviation (SD), whilst significance was set at $p \leqslant 0.05$. The EC_{50} values were obtained from full dose response curves, using a non-linear, dose response, curve fitting analysis *via* GraphPad Prism™ v.5 software and are summarized in Table 3.

3. Results

3.1. Chemistry

Condensation of dihydroartemisinin with 2-bromoethanol produced the DHA-ethyl bromide derivative **1** in good yield. The stereochemistry of this compound had previously been determined by our research group through X-ray analysis (Lombard et al., 2010). The configuration at C-10 stereocenter is assigned based on the vicinal coupling constant $J_{H\text{-}9:H\text{-}10}$ (Venugopalan et al., 1995). A large coupling constant (7–10 Hz) is generally found for

the 10α-isomer (Lin et al., 1997), indicating the relative *trans*-configuration. The 10β-isomer, indicating *cis*-configuration at C-10, on the other hand, has a smaller coupling constant (3.6–5 Hz) (Lin et al., 1989).

This intermediate and the final artemisinin–acridine hybrids **7–9** and **11** were therefore all in the 10β form, as confirmed by the small coupling constant, $J = 3.4–3.7$ Hz between the H-10 and H-9 atoms. The hybrid **10**, on the contrary, is a racemate mixture of both the 10α and 10β forms, as can be observed from the doublet of doublet (dd) with $J_{H9–H10}$ values of 3.5 Hz (10β) and 7.2 Hz (10α).

The 9-aminoacridine intermediates **2–6** were also prepared in low to high yields (45–79%) through nucleophilic substitution of the reactive chlorine in position 9 of 6,9-dichloro-2-methoxyacridine, with various amines by using the literature adapted method by Ishikawa et al. (2001). The IR spectra of these intermediates commonly showed absorption bands in the 3500–3200 cm^{-1} region, evident of the presence of both NH_2 and NH groups in their structures. Each amino-functionalized acridine intermediate was reacted with compound **1** through nucleophilic substitution, using microwave radiation (Scheme 1) to render a free base artemisinin–acridine hybrid. The hybrids **7–11** were obtained with yields in the 10–75% range.

The IR spectra of hybrids **7**, **8** and **11** displayed shoulders in the 3500–3300 cm^{-1} region, assignable due to the vibrations of secondary (N–H), while compounds **9** and **10** showed broad bands in the 1210–1150 cm^{-1} region, as a result of the presence of tertiary amine groups in their structures. A sharp band, corresponding with the stretching of the C–O bond of the endoperoxide bridge was also present in the 2950–2900 cm^{-1} region of the spectra of all hybrids, confirming the presence of the artemisinin moiety in these structures.

3.2. Physicochemical properties

Three different techniques were used to determine the physicochemical properties of the prepared compounds. These included DSC, which was used to determine both the physical state of the hybrids and their different transition phases. The TGA, on the other hand, served to determine the thermal stability of the compounds. Calculated ADMET properties, such as log*P*, solubility, absorption and BBB levels were determined to investigate the compounds' drug-likeness properties.

Due to the reported instability of the artemisinin class of antimalarials (Boreen et al., 2003; Lin et al., 1985), DSC and TGA were used to explore as to whether the addition of the 9-aminoacridine intermediate would have the ability to impart more stability onto the artemesinin pharmacophore. The hybrid compounds showed exceptional stability with a 9–14% weight loss in comparison with the 87% of DHA at 240 °C (Table 1).

Hybrids **7** and **10** displayed small endothermic phase transitions, with onset temperatures of 60.5 °C and 58.3 °C, respectively, which were consistent with glass transitions. Hybrid **11**, on the other hand, had two onset temperatures, *viz.* 58.5 °C and 102.6 °C, an indication that the equilibrium in phase transition was inadequate at lower temperature and that another cooperative molecular motion was required for internal re-adjustments (Souda, 2012). The rubberlike characteristics of compound **11** were more pronounced after the second phase transition.

Overall, the DSC thermograms suggested that all of the compounds **7–11** possessed amorphous structures.

Preliminary ADMET calculations were performed in order to determine the drug-likeness properties of the synthesized compounds.

The 9-aminoacridines **2–6**, with predicted logP values between 3 and 4 were more hydrophilic, compared to their respective hybrids **7–11**, with log*P* values in the 6–7.5 range (Table 2). These values were consistent with the intermediates and hybrids possessing low and extremely aqueous solubility levels. The amines also had better predicted human intestinal absorption and BBB penetration abilities than the hybrids.

The synthesized hybrids have a secondary/tertiary amino group that is the nitrogen N point linked to C-b and connecting both artemisinin and acridine pharmacophores. This N is for most compounds, the most basic with a calculated pK_a value ~9 therefore will not protonate at the physiological pH of 7.4. It is, however, likely to be protonated in an acidic environment, such as that occurring in the malaria parasite digestive vacuole.

3.3. In vitro antimalarial activity and cytotoxicity

The biological activities are summarized in Table 3.

The synthesized compounds were all active against both the NF54 and Dd2 strains. However, they were more active against NF54, than against the Dd2 strain, with resistance index (RI) values in the 2–19 range. The 9-aminoacridines **2–6** were less active than their corresponding hybrids, irrespective of the strain considered. All compounds were also found less potent than DHA and AS against both strains, while possessing either comparable or higher potencies than CQ. 9-Aminoacridine **4** and its corresponding hybrid **9** were the least active, while hybrids **7** and **10** were the most and second most active compounds, respectively.

All compounds were less cytotoxic than emetine against the CHO cells. The hybrids **7–11** appeared less toxic to CHO cells than their corresponding 9-aminoacridine intermediates, resulting in selective antimalarial action against the parasitic cells, with SI > 90, as compared to SI < 70 for the intermediates **2–6**. The anticancer activity picture against the HeLa cells was different. Indeed, all synthesized compounds were found to be more potent than CQ and melphalan, while showing lesser potency than both DHA and AS. In particular, hybrids **7** and **10** were found to be 3- and 8-, and 5- and 12-fold more potent than CQ and melphalan, respectively. The intermediates **2** and **4** showed less toxicity than their corresponding hybrids **5** and **9**, respectively, whereas the opposite was observed for compounds **3** and **6**, compared to their hybrids, **8** and **11**, respectively.

All synthesized compounds (except **5**), CQ, DHA and AS showed comparable apoptotic activity against both HepG2 and SH-SY5Y cell lines.

4. Discussion

4.1. Chemistry

The artemisinin–acridine hybrids were synthesized using microwave radiation. The peroxide bridge of artemisinin is reported to be prone to simplistic hydrolysis under basic or acidic conditions, and can also be expected to be heat sensitive (Torok and Ziffer, 1995). However, in this study, the spectroscopic data revealed no deviations from the expected values, confirming that this bridge was preserved during microwave radiation, which was in accordance with previous findings (Cloete et al., 2012).

In intermediates **2**, **3** and **6**, the secondary amine (NH) of the linkers was rendered less nucleophilic as a result of the resonance of the acridine ring, making it unavailable for substitution reactions. Subsequently, only the terminal, primary amine (in **2**) and secondary amine (in **3** and **6**) were involved in the substitution reactions, leading to the formation of hybrids **7**, **8** and **11**. The intermediate **4** (also **5**) has a tertiary amine, which is a group non-susceptible to nucleophilic substitution. Subsequently, only the secondary amine of the piperazine linker was involved in the reaction with **1** to form hybrid **9** (and **10**).

Substitution on the methyl-piperazine linker transpired on N-11 as a result of steric hindrance of the methyl group on C-13 and impeded the accessibility of N-16 for nucleophilic substitution to yield **5**.

Even though C-13 was a racemate, no indication of carbon splitting was observed on the ^{13}C NMR. The NMR data ensuing artemisinin–acridine hybrid **10**, however, displayed the presence of stereoisomers.

Furthermore, free base artemisinin-quinoline hybrids, previously synthesized by Lombard et al. (2011), using the same linkers, were found unstable, with very short shelf-lives after purification and isolation, causing them to thus convert into oxalate salts. No such instability was experienced among the artemisinin–acridine hybrids during this study, presumably due to the bulkiness and rigidity of the acridine ring. These compounds were therefore subjected to further investigations, namely physicochemical properties determinations and their *in vitro* biological evaluations as free bases.

Characteristic signals, indicative of the 9-aminoacridine portion of the artemisinin–acridine hybrids, represented the tricycle aromatic scaffold of the 9-aminoacridines with six-aryl protons, with integration signals ranging between δ 8.26–7.07 ppm and 3.91–3.98 ppm for protons H-1′, H-3′, H-4′, H-5′, H-7′, H-8′.

The protons for **7–11** on positions a, 4, 5, 7 and 8 were non-equivalent, splitting into an AB pattern for H-a, H-4, H-5, H-7, H-8 as follows: δ 4.13–3.88 (aα), 3.77–3.55 (aβ), 2.44–2.23 (4α), 2.07–1.91 (4β), 1.75–1.59 (5α), 1.62–1.13 (5β), 1.53–0.78 (7α, 7β), 1.94–1.53 (8α) and 1.53–1.00 (8β) ppm. The characteristic protons of H-b gave signals at δ 3.03–2.73 ppm. The protons on positions H-a, H-b and H-5 underwent chemical shifts upfield, due to the substitution of bromine with an electron donating amine. The protons on H-b of compound **7** were adjacent to a secondary amine and showed a chemical shift of 3.03 ppm (3.53 ppm for **1**), whereas **8** and **9**, adjacent to tertiary amines, reported chemical shifts of 2.79 ppm and 2.88 ppm, respectively.

For all hybrid compounds the proton on H-9 gave a characteristic doublet of quartets of doublets signal at δ 2.73–2.55 ppm, while the protons of H-12 resulted in a singlet and H-10 in a doublet, giving signals at δ 5.52–5.33 ppm and 4.86–4.77 ppm, respectively.

The most characteristic ^{13}C NMR signals were C-3, C-10, C-12, C-12a, C-a, C-b and C-9, at δ 104.13–104.03, 102.59–101.97, 87.99–87.88, 81.09–80.92, 67.73–63.34, 58.25–48.49 and 30.82–30.71 ppm, respectively. The hybrid carbons 3, 10, 12, 12a and 9 underwent no major chemical shifts with regards to **1**. The resultant chemical environment of C-a and C-b in the artemisinin–acridine hybrid led to C-a shifting upfield but C-b shifting downfield.

Furthermore, with the exception of compound **10**, in all other hybrid compounds only one isomer (10β) was observed. A mixture of isomers for **10** (10α and 10β) was confirmed by NMR data. This substantiated the racemic nature of the 3-methylpiperazin linker. In all of these structures, the theoretical number of alkyl groups in the linker was in accordance with that of DEPT135. COSY, HSQC and DEPT135, which further indisputably, indicated the presence of artemisinin and acridine moieties. These observations were validated by HRMS data.

4.2. Physicochemical/pharmacokinetic properties

The stability of drugs in general plays a fundamental role in ensuring their safety and potency, long after the manufacturing date. The stability of antimalarial drugs is impeded by economic and climatic factors in malaria endemic countries, where high heat and humidity conditions prevail (Brown, 2010) and storage facilities generally are inadequate. In this context, the hybrids during this study were subjected to TGA and DSC in order to establish whether they would be able to withstand the demanding thermodynamic conditions, occurring in the generally tropical, malaria endemic countries. The TGA data of **7–11** revealed weight losses between 9% and 14% at an extreme temperature of 240 °C, in contrast to the total degradation of DHA at the same temperature. DSC data revealed that compounds **7**, **10** and **11** underwent endothermic phase transitions, characteristic of a glass transition and possessed amorphous structures. Overall, hybrids **7–11** had minimum weight losses, with predictable proven stability in extreme conditions to withstand those harsh conditions prevailing in the malaria endemic countries.

Antimalarial drug research and development are furthermore affected by the pharmacokinetic and toxic profiles of potential compounds (Na-Bangchang and Karbwang, 2009). The physicochemical properties of antimalarial drugs are important in the sense that they can either help improve dose regimens and clinical efficiency, or encumber them. The importance of favourable solubility and absorption levels are paramount in increasing the plasma bioavailability, ensuring positive therapeutical responses (Ades, 2011) and are imperative in achieving the recommended >95% cure rate (Nosten and White, 2007).

The pharmacokinetic limitations of artemisinin had led to the development of synthetic and semi-synthetic derivatives to overcome its poor water solubility, absorption and bioavailability (Crespo-Ortiz and Wei, 2012). Since most antimalarial drugs are administrated orally, water solubility is necessary to ensure absorption and therapeutically viable plasma drug concentrations (Kasim et al., 2004). A high degree of water solubility is associated with hydrophilic compounds, allowing optimum absorption, whereas lipophilic compounds have low water solubility, but a high degree of cell permeation. Novel antimalarial compounds should hence possess balanced hydrophilic/lipophilic properties to permeate biological cell membranes and barriers to ensure predicable systemic drug concentrations (Avdeef, 2001).

The *n*-octanol/water partition coefficient (LogP) and aqueous solubility level provide predictable solubility characteristics in aqueous and organic solvents, with values between 1–5 being targeted and 1–3 being ideal for maximum absorption (Caron et al., 1999; Lipinski et al., 2001). The aqueous solubility level had been derived from a predictive model, generated from a comprehensive dataset by Cheng and Merz (2003) at 25 °C and pH 7 mimicking human blood, while the calculated human intestinal absorption model had been developed by incorporating various descriptors (Egan et al., 2000). Combined exploration of the log*P*, aqueous solubility level, absorption level and BBB penetration resulted in intermediates **2–6** exhibiting log*P* values in the targeted range, i.e. low solubility and good absorption, but high to medium blood brain penetration. Differences in the chain length or addition of secondary and tertiary amines had no definitive effect on the calculated drug-likeness properties of solubility and absorption, but increased BBB penetration of these 9-aminoacridine.

The corresponding artemisinin–acridine hybrids **7–11**, however, displayed high log P values, ranging across the limits of both the targeted and ideal ranges, i.e. extreme to very low solubility levels, very low-to-low absorption levels and undefined BBB penetration levels. All of the hybrids therefore possessed unfavourable drug-likeness properties. The undesirable logP values and solubility and absorption levels at physiological conditions could be attributed to blocking of the polar primary/secondary amine groups in the intermediates, causing a reduction in the hydrogen bonding formation, and the addition of the lipophilic artemisinin moiety.

The artemisinin–acridine hybrids had no predicted physicochemical/pharmacokinetic benefits over their precursor, 9-aminoacridines and therefore were expected to be biologically less active. However, since log*P* values, solubility and absorption levels, and other factors as a whole (rather than a single property) affect the

extent of a compound's ability to cross biological membranes and absorption into the systemic circulation (Bigucci et al., 2008), both intermediate and hybrids may have contracting biological activity profiles.

4.3. In vitro biological evaluation

The compounds were screened against the *P. falciparum* strains NF54 and Dd2. NF54 is a strain of *P. falciparum* from African origin that is susceptible to all known antimalarial drugs, and it is often the strain of choice to test for antigametocytocidal activity, presumably because of the highest gametocytemia obtained with this strain in cell cultures (Roncales et al., 2012). Contrary, the Dd2 strain is collected in Indochina/Laos, it is CQ and mefloquine resistant and delivers poor levels of gametocytemia in cultures (Roncales et al., 2012).

Plasmodium gametocytes, responsible for malaria parasite transmission from humans to mosquitoes, represent a crucial target for future new antimalarial drugs, in order to achieve malaria eradication.

Artemisinin and acridine pharmacophores are known to be active against malaria parasites (O'Neill et al., 2010; Valdés, 2011). *In vivo*, most artemisinin derivatives are within a few minutes metabolized into DHA (Grace et al., 1997; Karbwang et al., 1997; Woodrow et al., 2005). Arthemether and arteether, both ether derivatives of artemisinin, stay intact long enough to exercise their own antimalarial effect before being metabolized into DHA, with all three drugs showing comparable potencies (Woodrow et al., 2005). The synthesized hybrids also being ethers, will likewise exert their own antimalarial activities prior to metabolism into DHA, which is unlikely to occur *in vitro*. The reported IC_{50} values were therefore intrinsic to the hybrids, rather than due to any active metabolite.

The trend of ADMET predicted drug-likeable factors did not corroborate that of antimalarial activity, since 9-aminoacridines **2–6**, with more favourable predicted properties, displayed less activity than their corresponding hybrids. These results are therefore in agreement with previous reports that properties, such as hydrogen-bonding, molecular size and shape, polarity, flexibility and the charge/ionization of a compound/drug molecule as a whole (rather than a single property) affect its absorption through membranes (Bigucci et al., 2008).

Compounds **2–11** had primary, secondary and/or tertiary amine groups with calculated pK_a (ACD/ChemSketch, 2000) values being in the 8–10 range. Compound **4** and its corresponding hybrid **9** were the least active compounds against both strains. They possess a tertiary amine with calculated pK_a value of 9.37, while hybrid **7**, the most active compound, has a secondary amine with pK_a value of 8.45. Hybrid **7** is thus less basic than **9**, and yet more active. One of the mechanisms suggested to could explain the antimalarial activity of basic drugs, such as CQ (pK_a 10.2), is ion trapping, which relies on the protonation of weakly basic amino groups. Indeed, in the normal *in vivo* environment at pH 7.4, amines tend to be neutral and unprotonated, making it easy for them to cross lipophillic membranes. Upon reaching the acidic food vacuole of the malaria parasite, where the pH value is in the 4.5–5.5 range, these amines become protonated, making them less membrane permeable. The net effect of this mechanism is the increased accumulation of these amines in the digestive vacuole, giving rise to an increase in activity (Egan, 2003; Hindley et al., 2002). This observation may thus imply that, unlike with CQ, ion trapping may not play a significant role in the activities of these amino group containing compounds.

The mechanism of resistance of the Dd2 strain is still not completely elucidated. However, it has been shown that CQ-resistant including Dd2 parasites expel much more rapidly the CQ from the red blood cell (RBC) than CQ-sensitive parasites, and many observations indicated that a *P. falciparum* trans-membrane protein (PfCRT) is involved in this efflux (Sanchez et al., 2003; Howard et al., 2001; Wellems, 2002).

The majority of the synthesized intermediates and hybrids were found active against the NF54 strain, with significant losses in activity against Dd2, which resulted in high RI values in the 2–19 range. This is in accordance with the above previous finding. The hybrids showing different level of activity against the Dd2 strain suggest a difference in efflux level as a result of the difference in absorption through the cellular membrane. These values above 1 underlined the inability of the compounds to overcome resistance against Dd2. No such activity loss was experienced with DHA though. The combined analysis of the activity data of compounds **2–11** and DHA hence suggested that the presence of the acridine moiety had antagonized the activity of artemisinin, and that the hybrid strategy might not be the best option when wishing to achieve synergistic activity from these antimalarial pharmacophores.

Furthermore, compound **7**, the most active hybrid, showed a six-fold higher activity loss against the CQR strain, compared to **10** (RI: 13.6 *vs.* 2.4), the second most active compound. However, hybrid **7** displayed six times more activity than **10** against the NF54 strain. Gametocytes are responsible for malaria transmission from human to mosquitoes. Thus, a potentially effective and efficient antimalarial drug candidate should have the ability to completely eliminate gametocytes from the parasite's life cycle. Therefore, despite the higher RI value, the hybrid **7** appears a more promising antimalarial drug candidate than **10**.

The previously used acridine based antimalarial drug, *viz.* mepacrine, had been abandoned due to reported toxicity. Hepatotoxicity of acridine and neurotoxicity of DHA have also been reported (Grace et al., 1997). An attempt to ascertain whether the synthesized artemisinin–acridine hybrids could convey the same properties as the parent drugs, led in this study to screen all compounds **2–11** for their cytotoxicity and apoptotic activity against various mammalian cell line types of both animal and human origins. These included CHO (Chinese hamster ovarian, animal), HeLa (cervical cancer, human), HepG2 (hepatocellular carcinoma, human) and SH-SY5Y (neuroblastoma, human) cell lines. The latter cells are often used as *in vitro* models of neuronal function and differentiation and are therefore a viable cell line to investigate neurotoxic properties of compounds.

Analysis of the IC_{50} values revealed all compounds to be more toxic to the mammalian cell line of animal origin (lower IC_{50} against CHO), than to those of human origin. The 9-aminoacridines **2–6** were more cytotoxic to CHO and were found to be less selective in their antimalarial actions against the parasitic cells (lower SI values), than were hybrids **7–11**, DHA, AS and CQ. This suggested that the presence of the artemisinin pharmacophore had contributed in reducing the cytotoxicity of the acridine moiety against the CHO cells in the hybrids.

The majority of hybrids appeared less cytotoxic than DHA, but displayed more toxicity than their precursor 9-aminoacridines against the HeLa cells, indicating that covalently linking acridine and artemisinin pharmacophores had led to a reduction in the cervical anticancer activity of the latter. Antagonism of anticaner activity, using the hybrid strategy, therefore occurred.

All synthesized compounds (except **5**) were found to be as apoptotic as DHA, AS and CQ against the HepG2 and SH-SY5Y cells. This indicated that both acridine and artemisinin pharmacophores had transferred their hepatotoxicity and neurotoxicity characteristics over into the hybrids although these properties were less expressed than the cytotoxicity and anticancer activity against CHO and HeLa cells, respectively.

On account of activity, resistance index, selectivity and cytotoxicity/apoptosis, hybrid **7** stood as a possible future antimalarial drug candidate while hybrid 10 may stand for possible exploration as an anticancer drug.

5. Conclusion

In this study, novel 9-aminoacridines and artemisinin–acridine hybrids were synthesized in one- and three step synthetic routes, respectively. All structures were confirmed by means of NMR, HRMS and IR techniques. The 9-aminoacridines displayed better ADMET predicted drug-likeness than their corresponding hybrids. However, in screens alongside DHA, AS and CQ, although both compound types were active against the NF54 and Dd2 strains of *P. falciparum*, the hybrids possessed higher activity than their precursor 9-aminoacridines. No resistance against the CQR strain Dd2 was overcome during this study, since all synthesized compounds had lost their activities against that strain in comparison with NF54. The majority of hybrids showed more antimalarial potency than CQ, but less than DHA and AS against both strains. They were more selective in their antiparasitic actions. The hybrids displayed better anticancer activity than the aminoacridines and CQ, but less than both DHA and AS. All synthesized and reference drugs possessed comparable hepatotoxicity and neurotoxicity.

Hybrid **7**, containing ehtylenediamine linker, was the most promising antimalarial compound synthesized during this study. It had 7-fold higher antimalarial potency than of CQ against both the NF54 and Dd2 strains, with high selective action towards the parasitic cells. Hybrid **7** also demonstrated anticancer activity against the HeLa cell line with 3- and 5-fold higher activity in comparison with CQ and melphalan, respectively. Hybrid **10** which features 2-methylpiperazin linker, showed more favourable anticancer than antimalarial property, being 5- and 12-fold more potent than CQ and melphalan, respectively. This compound may therefore stand as drug candidate for further investigation in search for new anti-cervical cancer drugs, rather than malaria.

In summary, the hybrid strategy did not lead to reducing the toxicity of the acridine moiety, nor was resistance of the malaria parasites to chloroquine overcome. No synergistic activities were obtained by combining artemisinin and acridine pharmacophores. The hybrid strategy during this study had therefore resulted in limited benefits.

Disclaimer

Any opinions, findings and conclusions or recommendations expressed in this material are those of the author(s) and therefore the NRF does not accept any liability in regard thereto.

Acknowledgements

This work was based upon research financially supported by the National Research Foundation (NRF) and the North-West University. The authors thank Dr. J.H.L. Jordaan for MS analysis, Mr. A. Joubert for NMR analysis, Prof. W. Liebenberg for TGA and DSC and Prof. M. van de Venter and Ms. M.C. Pruissen for cytotoxicity screening.

Appendix A. Supplementary material

Supplementary data associated with this article can be found, in the online version, at http://dx.doi.org/10.1016/j.ejps.2014.01.014.

References

Ades, V., 2011. Safety: pharmacokinetics and efficacy of artemisinins in pregnancy. Infect. Dis. Rep. 3 (37), 43.
Advanced Chemistry Inc. ACD/ChemSketch, 2000, Version 4.5.
Amuasi, J.H., Diap, G., Nguah, S.B., Karikari, P., Boakye, I., Jambai, A., Lahai, W.K., Louie, K.S., Kiechel, J.R., 2012. Access to artemisinin-combination therapy (ACT) and other anti-malarials: national policy and markets in Sierra Leone. PLoS ONE 7, e47733.
Avdeef, A., 2001. Physicochemical profiling: solubility, permeability and charge state. Curr. Top. Med. Chem. 1, 277–351.
Berman, J., Brown, L., Miller, R., Andersen, S.L., McGreevy, P., Schuster, B.G., Ellis, W., Ager, A., Rossan, R., 1994. Antimalarial activity of WR 243251: a dihydroacridinedione. Antimicrob. Agents Chemother. 38, 1753–1756.
Biagini, G.A., Fisher, N., Berry, N., Stocks, P.A., Meunier, B., Williams, D.P., Bonar-Law, R., Bray, P.G., Owen, A., O'Neill, P.M., Ward, S.A., 2008. Acridinediones: selective and potent inhibitors of the malaria parasite mitochondrial *bc*1 complex. Mol. Pharmacol. 73, 1347–1355.
Bigucci, F., Kamsu-Kom, T., Cholet, C., Besnard, M., Bonnet-Delpon, D., Ponchel, G., 2008. Transport of fluoroalkyl dihydroartemisinin derivatives across rat intestinal tissue. J. Pharm. Pharmacol. 60, 163–169.
Boreen, A.L., Arnold, W.A., McNeill, K., 2003. Photodegradation of pharmaceuticals in the aquatic environment: a review. Aquat. Sci. 65, 320–341.
Brown, G.D., 2010. The biosynthesis of artemisinin (qinghaosu) and the phytochemistry of *Artemisia annua* L. (qinghao). Mol. Pharmacol. 15, 7603–7698.
Burgess, S.J., Selzer, A., Kelly, J.X., Smilkstein, M.J., Riscoe, M.K., Peyton, D.H., 2006. A chloroquine-like molecule designed to reverse resistance in *Plasmodium falciparum*. J. Med. Chem. 49, 5623–6525.
Capela, R., Cabal, G.G., Rosenthal, P.J., Gut, J., Mota, M.M., Moreira, R., Lopes, F., Prudêncio, M., 2011. Design and evaluation of primaquine–artemisinin hybrids as a multi-stage antimalarial strategy. Antimicrob. Agents Chemother. 55, 4698–4706.
Caron, G., Raymond, F., Carrupt, P.A., Girault, H.H., Testa, B., 1999. Combined molecular lipophilicity descriptore and their role in understanding intramolecular effects. Pharm. Sci. Technol. Today 2, 327–335.
Cheng, A., Merz, Z.P., 2003. Prediction of aqueous solubility of a diverse set of compounds using quantitative structure–property relationships. J. Med. Chem. 46, 3572–3580.
Ciesielska, E., Pastwa, E., Szmigiero, L., 1997. Inhibition of mammalian topoisomerase I by 1-nitro-9-aminoacridines: dependence on thiol activation. Acta Biochim. Pol. 44, 775–780.
Cloete, T.T., Breytenbach, J.W., de Kock, C., Smith, P.J., Breytenbach, J.C., N'Da, D.D., 2012. Synthesis, antimalarial activity and cytotoxicity of 10-aminoethylether derivatives of artemisinin. Bioorg. Med. Chem. 20, 4701–4709.
Crespo-Ortiz, M.P., Wei, M.Q., 2012. Antitumor activity of artemisinin and its derivatives: from a well-known antimalarial agent to a potential anticancer drug. J. Biomed. Biotechnol. 2012, 247597.
Egan, T.J., 2003. Haemozoin (malaria pigment): a unique crystalline drug target. Targets 2, 115–124.
Egan, W.J., Merz, K.M., Balwin, J.J., 2000. Prediction of drug absorption using multivariate statistics. J. Med. Chem. 43, 3867–3877.
Elueze, E.I., Croft, S.L., Warhurst, D.C., 1996. Activity of pyronaridine and mepacrine against twelve strains of *Plasmodium falciparum in vitro*. J. Antimicrob. Chemother. 37, 511–518.
Fairhurst, R.M., Nayyar, G.M., Breman, J.G., Hallett, R., Vennerstrom, J.L., Duong, S., Ringwald, P., Wellems, T.E., Plowe, C.V., Dondorp, A.M., 2012. Artemisinin-resistant malaria: research challenges, opportunities and public health implications. Am. J. Trop. Med. Hyg. 87, 231–241.
Fink, G., Dickens, W.T., Jordan, M., Cohen, J.L., 2013. Access to subsidized ACT and malaria treatment-evidence from the first year of the AMFm program in six districts in Uganda. Health Policy Plan., 1–11.
Global Malaria Action Plan, 2013. <www.rbm.who.int/gmap/gmap.pdf> (date of access: 20.04.13).
Gregson, A., Plowe, C.V., 2005. Mechanisms of resistance of malaria parasites to antifolates. Pharmacol. Rev. 57, 117–145.
Grace, J.M., Aguilar, A.J., Trotman, K.M., Peggins, J.O., Brewer, T.G., 1997. Metabolism of β-arteether to dihydroqinghaosu by human liver microsomes and ecombinant cytochrome P450. Drug Metab. Dispos. 26, 313–317.
Hindley, S., Ward, S.A., Storr, R.C., Searle, N.L., Bray, P.G., Park, B.K., Davies, J., O'Neill, P.M., 2002. Design and synthesis of endoperoxide antimalarial prodrug models. J. Med. Chem. 45, 1052–1063.
Howard, E.M., Zhang, H., Roepe, P.D., 2001. A novel transporter, Pfcrt, confers antimalarial drug resistance. J. Membr. Biol. 190, 1–8.
Hulsman, N., Medema, J.P., Bos, C., Jongejan, A., Leurs, R., Smit, M.J., De Esch, I.J., Richel, D., Wijtmans, M., 2007. Chemical insights in the concept of hybrid drugs: the antitumor effect of nitric oxide-donating aspirin involves a quinone methide but not nitric oxide nor aspirin. J. Med. Chem. 50, 2424–2431.
Ibrahim, B., Sowemimo, A., Spies, L., Koekomoer, T., van de Venter, M., Odukoya, O.A., 2013. Antiproliferative and apoptosis inducing activity of *Markhamia tomentosa* leaf extract on HeLa cells. J. Ethnopharmacol. 149, 745–749.
Ishikawa, Y., Yamashita, A., Uno, T., 2001. Efficient photocleavage of DNA by cationic porphyrin–acridine hybrids with the effective length of diamino alkyl linkage. Chem. Pharm. Bull. (Tokyo) 49, 287–293.
Karbwang, J., Na-Bangchang, K., Congpuong, K., Molunto, P., Thanavibul, A., 1997. Pharmacokinetics and bioavailability of oral and intramuscular artemether. Eur. J. Clin. Pharmacol. 52, 307–310.
Kasim, N.A., Whitehouse, M., Ramachandran, C., Bermejo, M., Lennernäs, H., Hussain, A.S., Junginger, H.E., Stavchansky, S.A., Midha, K.K., Shah, V.P., Amidon, G.L., 2004. Molecular properties of WHO essential drugs and provisional biopharmaceutical classification. Mol. Pharm. 1, 85–96.
Lai, H.C., Singh, N.P., Sasaki, T., 2013. Development of artemisinin compounds for cancer treatment. Invest. New Drugs 31, 230–246.
Li, Y., Zhu, Y.M., Jiang, H.J., Pan, J.P., Wu, G.S., Wu, J.M., Shi, Y.L., Yang, J.D., Wu, B.A., 2000. Synthesis and antimalarial activity of artemisinin derivatives containing an amino group. J. Med. Chem. 43, 1635–4043.

Lipinski, C.A., Lombardo, F., Dominy, B.W., Feeney, P.J., 2001. Experimental and computational approaches to estimate solubility and permeability in drug discovery and development settings. Adv. Drug Deliv. Rev. 46, 3–26.
Lombard, M.C., Fernandes, M.A., Breytenbach, J.C., N'Da, D.D., 2010. 1-Bromo-2-(10β-dihydroartemisinoxy)-ethane. Acta Crys. E. 66, 2182–2183.
Lombard, M.C., N'Da, D.D., Jaco, C., Breytenbach, J.C., Smith, P.J., Lategan, C., 2011. Synthesis and antimalarial activity of artemisinin-quinoline hybrids. Bioorg. Med. Chem. Lett. 21, 1683–1686.
Lin, A.J., Klayman, D.L., Hoch, J.M., Silverton, J.V., George, C.F., 1985. Thermal rearrangement and decomposition products of artemisinin (qinghaosu). J. Org. Chem. 50, 4504–4508.
Lin, A.J., Zikry, A.B., Kyle, D.E., 1997. Antimalarial activity of new dihydroartemisinin derivatives. 7. 4-(p-Substituted phenyl)-4 (R or S)-[10 (α or β) dihydroartemisininoxy] butyric acids. J. Med. Chem. 40, 1396–1400.
Lin, A.J., Lee, M., Klayman, D.L., 1989. Antimalarial activity of new water-soluble dihydroartemisinin derivatives: 2. Stereospecificity of the ether side chain. J. Med. Chem. 32, 1249–1252.
Makler, M.T., Ries, J.M., Williams, J.A., Bancroft, J.E., Piper, R.C., Gibbins, B.L., Hinrichs, D.J., 1993. Parasite lactate dehydrogenase as an assay for *Plasmodium falciparum* drug sensitivity. Am. J. Trop. Med. Hyg. 48, 739–741.
Meshnick, S.R., 2002. Artemisinin: mechanisms of action, resistance and toxicity. Int. J. Parasitol. 32, 1655–1660.
Meunier, B., 2008. Hybrid molecules with a dual mode of action: dream or reality. Acc. Chem. Res. 41, 69–77.
Mosmann, T., 1983. Rapid colorimetric assay for cellular growth and survival: application to proliferation and cytotoxicity assays. J. Immunol. Methods 65, 55–63.
Muregi, F.W., Ishih, A., 2010. Next-generation antimalarial drugs: hybrid molecules as a new strategy in drug design. Drug Dev. Res. 71, 20–32.
Na-Bangchang, K., Karbwang, J., 2009. Current status of malaria chemotherapy and the role of pharmacology in antimalarial drug research and development. Fundam. Clin. Pharmacol. 23, 387–409.
Njogu, P.M., Gut, J., Rosenthal, P.J., Chibale, K., 2013. Design, synthesis, and antiplasmodial activity of hybrid compounds based on (2R,3S)-N-benzoyl-3-phenylisoserine. ACS. Med. Chem. Lett. 4, 637–641.
Nosten, F., White, N.J., 2007. Artemisinin-based combination treatment of *Falciparum* malaria. Am. J. Trop. Med. Hyg. 77, 181–192.
O'Neill, P.M., Barton, V.E., Ward, S.A., 2010. The Molecular mechanism of action of artemisinin-the debate continues. Molecules 15, 1705–1721.
Pérez, B., Teixeira, C., Gomes, A.S., Albuquerque, I.S., Gut, J., Rosenthal, P.J., Prudêncio, M., Gomes, P., 2013. *In vitro* efficiency of 9-(*N*-cinnamoylbutyl)aminoacridines against blood- and liver-stage malaria parasites. Bioorg. Med. Chem. Lett. 23, 610–613.
Ploypradith, P., 2004. Development of artemisinin and its structurally simplified trioxane derivatives as antimalarial drugs. Acta Trop. 89, 329–342.
Price, R.N., 2013. Potential of artemisinin-based combination therapies to block malaria transmission. J. Infect. Dis. 207, 1627–1629.
Price, R.N., Nosten, F., Luxemburger, C., Ter Kuile, F.O., Paiphun, L., Chongsuphajaisiddhi, T., White, N.J., 1996. Effects of artemisinin derivatives on malaria transmissibility. Lancet 347, 1654–1658.
Roncales, M., Vidal-Mas, J., Leroy, D., Herreros, E., 2012. Comparison and optimization of different methods for the *in vitro* production of *Plasmodium falciparum* gametocytes. J. Parasitol. Res. 2012, 927148–927155.
Rubinstein, L.V., Shoemaker, R.H., Paull, K.D., Simon, R.M., Tosini, S., Skehan, P., Scudiero, D.A., Monks, A., Boyd, M.R., 1990. Comparison of *in vitro* anticancer-drug-screening data generated with a tetrazolium assay against a diverse panel of human tumor cell lines. J. Natl. Cancer Inst. 82, 1113–1118.
Rudrapal, M., 2011. A brief review on malaria and current antimalarial drugs. Curr. Pharm. Res. 1, 286–292.
Sanchez, C.P., Stein, W., Lanzer, M., 2003. Trans stimulation provides evidence for a drug efflux carrier as the mechanism of chloroquine resistance in *Plasmodium falciparum*. Biochemistry 42, 9383–9394.
Schlitzer, M., 2008. Antimalarial drugs: what is in use and what is in the pipeline. Arch. Pharm. Chem. Life Sci. 341, 149–163.
Souda, R., 2012. Roles of individual and cooperative motions of molecules in glass–liquid transition and crystallization of toluene. J. Phys. Chem. B 114, 10734–10739.
Torok, D.S., Ziffer, H., 1995. Synthesis and reactions of ll-azaartemisinin and derivatives. Tetrahedron Lett. 36, 829–832.
Trager, W., Jensen, J.B., 1976. Human malaria parasite in continuous culture. Science 193, 673–675.
Valdés, A.F.C., 2011. Acridine and acridinones: old and new structures with antimalarial activity. Open Med. Chem. J. 5, 11–20.
Venugopalan, B., Karnik, P.J., Bapat, C.P., Chatterjee, D.K., Iyer, N., Lepcha, D., 1995. Antimalarial activity of new ethers and thioethers of dihydroartemisinin. Eur. J. Med. Chem. 30, 697–706.
Walsh, J.J., Bell, A., 2009. Hybrid drugs for malaria. Curr. Pharm. 15, 2970–2985.
Walsh, J.J., Coughlan, D., Heneghan, N., Gaynor, C., Bell, A., 2007. A novel artemisinin–quinine hybrid with potent antimalarial activity. Bioorg. Med. Chem. Lett. 17, 3599–3602.
Wellems, T.E., 2002. *Plasmodium* chloroquine resistance and the search for a replacement antimalarial drug. Science 298, 124–126.
Winter, R.W., Kelly, J.X., Smilkstein, M.J., Dodean, R., Bagby, G.C., Keaney Rathbun, R., Levin, J.I., Hinrichs, D., Riscoe, M.K., 2006. Evaluation and lead optimization of anti-malarial acridones. Exp. Parasitol. 114, 47–56.
Woodrow, C.J., Haynes, R.K., Krishna, S., 2005. Artemisinins. Postgrad. Med. J. 81, 71–78.
World Health Organization (WHO), 2011. World Malaria Report 2011. <http://www.who.int/malaria/publications/atoz/9789241564403/en/index.html> (date of access: 20.04.13).
World Health Organization (WHO), 2012. World Malaria Report 2012. <http://www.who.int/malaria/publications/world_malaria_report_2012/report/en/index.html> (date of access: 20.04.13).
Xie, L., Zhai, X., Ren, L., Meng, H., Liu, C., Zhu, W., Zhao, Y., 2011. Design, synthesis and antitumor activity of novel artemisinin derivatives using hybrid approach. Chem. Pharm. Bull. (Tokyo) 59, 984–990.